



## Carbon Nanotubes Synthesized by Catalytic Chemical Vapour Deposition using Fe-Supported Zeolite<sup>†</sup>

WEI ZHAO<sup>1</sup>, DONG NAM SEO<sup>1</sup>, HYUN SUNG KIM<sup>2</sup>, HYUNG TAE KIM<sup>3</sup> and IK JIN KIM<sup>1,\*</sup>

<sup>1</sup>Institute for Processing and Application of Inorganic Materials (PAIM), Department of Materials Science and Engineering, Hanseo University, 360 Daegok-ri, Haemi-myun, Seosan City, Chungnam 356-706, South Korea

<sup>2</sup>Center for Nanomaterials/Korea Center for Artificial Photosynthesis (KCAP), Sogang Bldg., Sogang University, 1-3 Shinsu-dong, Mapo-gu, Seoul 21-854, South Korea

<sup>3</sup>Korea Institute of Ceramic Engineering and Technology(KICET), 30 Gyeongchung Rd, Sindun-myeon, Icheon-si, Gyeonggi-do 467-843, South Korea

\*Corresponding author: E-mail: ijkim@hanseo.ac.kr

AJC-9558

Multi-walled carbon nanotubes (MWNTs) were synthesized on Fe-supported zeolite by catalytic chemical vapour deposition (CCVD) using acetylene as the carbon source. Well-shaped zeolite NaX (FAU) octahedral crystals of a size of 15  $\mu\text{m}$  were synthesized hydrothermally in a mother solution with a composition of 3.5 Na<sub>2</sub>O : Al<sub>2</sub>O<sub>3</sub> : 2.1 SiO<sub>2</sub> : 1000 H<sub>2</sub>O. The effect of the iron content and the reaction time on the synthesis of carbon nanotubes (CNTs) was investigated through transmission electron microscopy (TEM), thermogravimetric analysis (TGA) and Raman spectroscopy. After 1 h reaction, quite a number of CNTs had inner and outer diameters both below 10 nm, which were smaller than those of conventional thick MWNTs. With increasing iron contents in the zeolite, the carbon yield shows a monotonic increasing tendency, reaching 52.9 % when the iron content is up to 6.72 wt. %. In addition, with prolonged reaction time, the inner diameter of the CNTs remained constant while the outer diameter became thicker and thicker, with the carbon yield after the reaction of 3 h reaching 58.2 %. Moreover, the CNTs obtained after much longer reaction time may have a weaker crystallinity.

**Key Words:** Carbon nanotubes, Catalytic chemical vapour deposition, Zeolite, Fe.

### INTRODUCTION

The discovery of carbon nanotubes (CNTs) by Iijima<sup>1</sup> has stimulated intensive studies to characterize their structure and to determine their properties both by direct measurement and predictive modeling techniques<sup>2,3</sup>. As known, they are cylindrical shells made by rolling graphene sheets, with the carbon atoms arranged in a honeycomb-like hexagonal structure<sup>4</sup> and are classified into two categories: single-walled carbon nanotubes (SWNTs) and multi-walled carbon nanotubes (MWNTs).

Because the varying twist degrees of their rolled-up graphene sheets along the length, CNTs can have a variety of chiral structures. Depending on their diameter and the helicity of the arrangement of graphitic rings in the walls, they have been demonstrated to possess unusual electronic, photonic, magnetic, thermal and mechanical properties<sup>2</sup>. Due to their unique physical and chemical properties<sup>5</sup>, they promise a variety of potential technological applications across many

fields such as energy storage media<sup>6</sup>, field emission devices<sup>7</sup>, nanoelectronic devices<sup>8</sup> and so on.

So far, for synthesizing CNTs, a variety of promising techniques such as arc-discharge<sup>1</sup>, laser ablation<sup>9</sup> and chemical vapour deposition (CVD)<sup>10</sup> have been developed. Because of the low system cost, simple operating conditions, easy control of experimental parameters and feasibility of exploring various carbon sources in solid, liquid and gas forms, CVD has been proven to be more efficient, especially the catalytic CVD (CCVD) method<sup>11</sup> offering great advantages, where CNTs are grown over catalysts containing nanoparticles of transition metal (Fe, Co, Ni) or related oxides by the decomposition of a carbon source (CH<sub>4</sub>, C<sub>2</sub>H<sub>2</sub>, C<sub>2</sub>H<sub>4</sub>, C<sub>2</sub>H<sub>5</sub>OH, *etc.*). Moreover, controlling the morphology of these particles during CNT growth is critical for nanotube characteristics such as thickness, uniformity and yield<sup>12</sup>. However, the problem is the fact that the metal particles down to nanometer scale tend to agglomerate. Therefore, porous supports or matrices such as zeolites<sup>13</sup>, mesoporous silica<sup>14</sup>, silica<sup>15</sup>, alumina<sup>16</sup> are required for contri-

<sup>†</sup>Presented to the 4th Korea-China International Conference on Multi-Functional Materials and Application.

buting to particle stabilization and producing a fine dispersion of well-defined particles, thus increasing nucleation sites advantageous to the synthesis of CNTs. Among them, zeolites, with the structural homogeneity<sup>17</sup>, high reactive surface area and pore diameters in the range of 3-10 Å, can be host candidates for different kinds of adsorbing molecules<sup>18</sup> and hence could be used as supports for catalyst particles to synthesize and grow CNTs.

In this work, the zeolite NaX (FAU) is used as the template to hold the catalysts for synthesizing CNTs by CCVD. With the careful characterization, the influence of different iron contents supported in the zeolite and the effect of reaction time on the synthesis of CNTs were investigated.

## EXPERIMENTAL

**Preparation of Fe-supported zeolite catalysts:** Zeolite NaX (FAU) crystals of 15 μm were synthesized hydrothermally in a mother solution with a composition of 3.5 Na<sub>2</sub>O : Al<sub>2</sub>O<sub>3</sub> : 2.1 SiO<sub>2</sub> : 1000 H<sub>2</sub>O. Afterwards, the synthesized zeolite powder (1 g) was refluxed with aqueous solutions of FeCl<sub>2</sub>·4H<sub>2</sub>O (≥ 99.0 %) at *ca.* 30-40 °C. The solutions were made by dissolving FeCl<sub>2</sub>·4H<sub>2</sub>O powder of different masses (0.04, 0.08, 0.12 mol %) in 250 mL deionized water. The mixture was then further centrifuged, washed thoroughly with pure ethanol (≥ 99.9 %) and dried at ambient temperature. The complete ion-exchanging of Fe<sup>2+</sup> cations could be verified by the colourless clear filtrate solution obtained after centrifugation. Finally, the calcination of the powder was performed at 450 °C for 3 h in air. For convenience, three catalyst samples were designated as FeNaX0, FeNaX1 and FeNaX2, with the iron content being *ca.* 2.23, 4.44 and 6.72 wt. %, respectively.

**Growth of carbon nanotubes:** The growth of CNTs was performed in a horizontal electric tubular furnace at atmospheric pressure with a thin layer of catalyst (100 mg) placed in a quartz boat in its center. In a typical synthesis experiment, the catalyst was heated from room temperature to 700 °C under the protection of a nitrogen flow (200 mL min<sup>-1</sup>) and kept at this temperature for about 15 min. Acetylene (10 mL min<sup>-1</sup>) was then introduced into the reactor to initiate the CNT growth. After a reaction of 1 h, the furnace was cooled down to room temperature under the protection of nitrogen flow. All gases were delivered into the furnace by using mass flow controllers. Three CNT samples were designated as CNT-FeNaX0, CNT-FeNaX1 and CNT-FeNaX2. Using the same process, the catalyst FeNaX2 was selected to synthesize CNTs for 0.5, 1.0, 2.0 and 3.0 h. These products were designated as CNT30, CNT60, CNT120 and CNT180.

**Characterization of products:** High resolution transmission electron microscopy (HRTEM) images were taken on a JEOL JEM-3011 at an accelerating voltage of 200 kV. Thermogravimetric (TG) test was conducted under air in a Seiko Extar 7300 (TG/DTA 7300) instrument, with samples of *ca.* 5 mg heated in air from 25 to 750 °C, at a heating rate of 10 °C/min. The Raman spectroscopy measurements were performed with a Raman system FRA-106/S using a laser excitation line at 1064 nm (Nd-YAG).

## RESULTS AND DISCUSSION

Fig. 1(c) shows the SEM image of synthesized zeolite crystals, presenting a homogeneity of them. Moreover, the TEM image (Fig. 1(a)) of them was taken which exhibits a high degree of structural order in the crystal surface formed inside

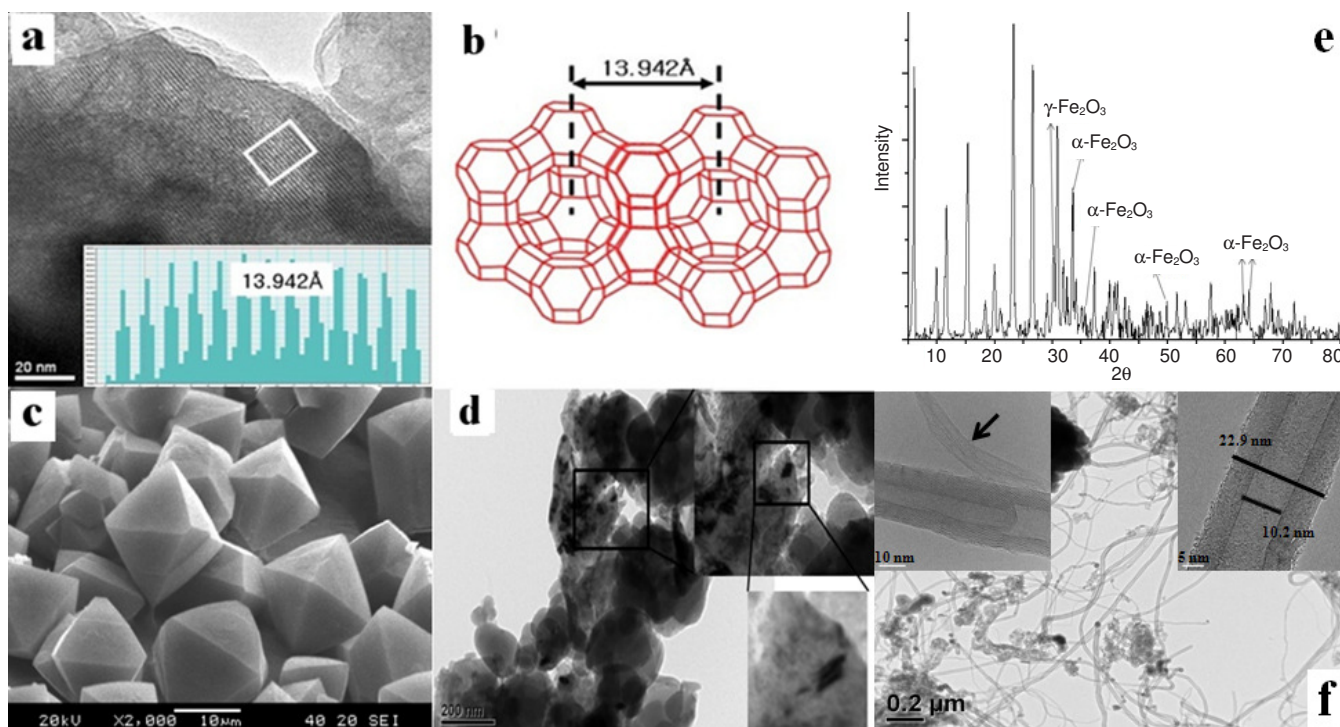


Fig. 1. (a) TEM image of the zeolite crystal, (b) Schematic structure of the zeolite crystal, (c) SEM image of zeolite crystals, (d) TEM image of the catalyst FeNaX2, (e) XRD pattern of the catalyst FeNaX2 and (f) TEM image of synthesized CNTs on FeNaX2



the complementary pores between two distinct peaks, each centered at 13.942, corresponding to the inner diameter of the zeolite structure, as shown in Fig. 1(b). As shown, zeolite (FAU) can be described as an ensemble of sodalite cages or  $\beta$ -cages joined hexagonal prisms, with the supercage whose diameter is of *ca.* 13 Å<sup>19</sup>.

After ion-exchanging and calcination, catalyst nanoparticles and some agglomeration of them [small black spots emphasized and shown in enlarged images in Fig. 1(d)] randomly dispersed in the zeolite are clearly evident and their main component was confirmed as  $\alpha$ -Fe<sub>2</sub>O<sub>3</sub> by XRD pattern as shown in Fig. 1(e), even though its content was too low to be easily observed. Moreover, the breakdown of the zeolitic structure after the calcination can be readily identified in Fig. 1(d) where the zeolitic crystal has been ruptured, containing irregularly shaped cavities with a size distribution in the range of mesopores.

For CNTs synthesized for 1 h shown in Fig. 1(f), it is clear to see they are MWNTs with some amorphous carbon on the outer wall of them and there are some black spots inside or around CNTs, indicating remaining catalyst particles. According to a previous study<sup>20</sup>, ambiguity still remains on what is the exact catalyst for the synthesis of CNTs. Through careful TEM investigations, there are two groups of CNTs with different diameter ranges, typically shown in the left inset of Fig. 1(f). One of them has some thinner CNTs with both inner and outer diameters below 10 nm [presented by the arrow in the left inset of Fig. 1(f)], much smaller than those synthesized by

conventional CVD method, which was already reported in previous work<sup>21</sup>. In addition, it could be seen that the CNTs could clearly be synthesized at low iron content and exhibited a growth tendency with increasing iron content. This suggests that with increasing iron content, more catalyst particles act as "seeds" for the CNT synthesis. Also, the other group of synthesized CNTs for 1 h has inner and outer diameters of 10.2± and 22.9± nm, respectively, which can be seen in the right inset of Fig. 1(f).

Fig. 2 exhibits HRTEM images of synthesized CNTs on the catalyst FeNaX2 for 0.5, 2.0 and 3.0 h, which are also MWNTs with some amorphous carbon on the outer wall of them. The reason for selecting this catalyst sample is the yield of CNTs catalyzed by it, which was demonstrated before<sup>21</sup>. Combined with the result of those for 1 h, they clearly show that the inner diameters of them are very close to 10 nm, without distinct changes and their outer diameters present a monotonic increase tendency with prolonged reaction time, which corresponds to increasing number of walls of synthesized CNTs, that is, 15, 19, 20 and 25 layers. This result indicates that carbon atoms decomposed from C<sub>2</sub>H<sub>2</sub> form coaxial cylindrical graphene sheets layer by layer around the core of CNTs with prolonged reaction time.

Despite that, the phenomenon that CNTs synthesized for 1 h show severe inhomogeneity needs to be further investigated. And our explanation is as follows. Even though the zeolite has been applied for finely dispersing and stabilizing them, the calcination broke the zeolitic structure to some extent. This

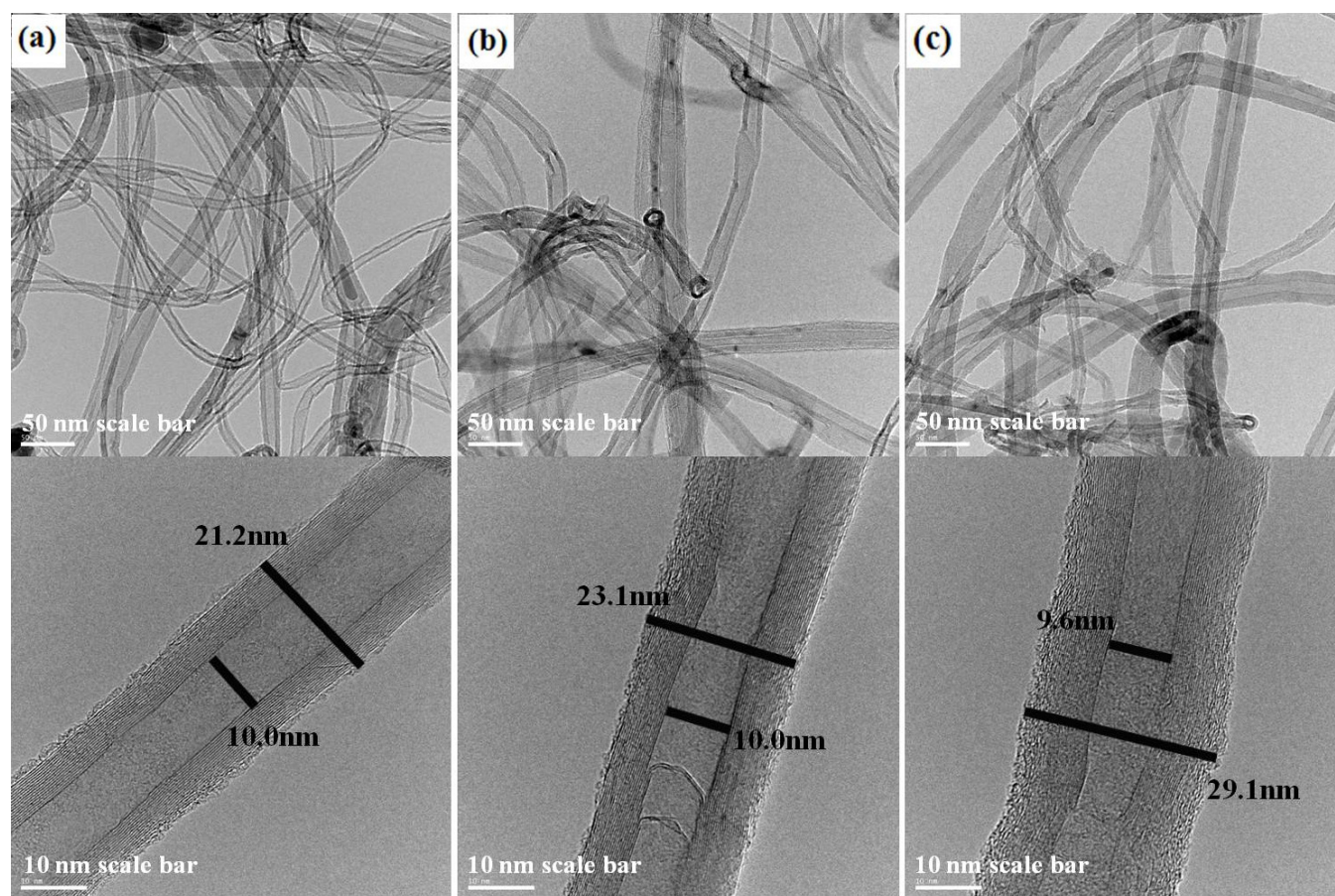


Fig. 2. TEM images of synthesized CNTs within different reaction time (a) CNT30, (b) CNT120 and (c) CNT180

could not avoid the agglomeration of catalyst particles, so that their size became inhomogeneous, leading to different diameter ranges of carbon nanotubes.

Thermogravimetric analysis was performed to measure the amount of carbon deposited in the experiment and also to evaluate the percentage of other forms of carbon. As reported by our previous work<sup>21</sup>, during the heating process, the products CNT-FeNaX0, CNT-FeNaX1 and CNT-FeNaX2 show an initial weight loss (*ca.* 280 °C) attributed to the loss of physically absorbed heavy water in the zeolite and a two-step weight loss due to combustion of amorphous carbon (350-500 °C) and MWNTs ( $\geq 500$  °C), respectively. Moreover, three samples exhibit a gradual increasing tendency of weight loss at the second combustion step, which implies that CNT production can be increased with increasing iron content supported in the zeolite. This result confirms the TEM analyses above.

In addition, Fig. 3 presents TG curves of CNT samples, CNT30, CNT60, CNT120 and CNT180. All of them present a similar three-step weight loss process, which comprises an initial loss of physically absorbed water in the zeolite, the first-step combustion of amorphous carbon species and the second-step combustion of synthesized MWNTs. It is apparent that there is some difference between the initial weight losses, which might generate from the natural error caused by using catalysts prepared in different batches despite the same method. According to the careful evaluation, there exist a decreasing trend of the amorphous carbon species and an increasing trend of the MWNT yield, which is in accordance with the TEM analysis. It is worth noting that the burning temperature (*ca.* 490 °C) of the MWNTs in our work is much lower than that of the generally thick MWNTs (*ca.* 700 °C) grown by CVD method<sup>22</sup>.

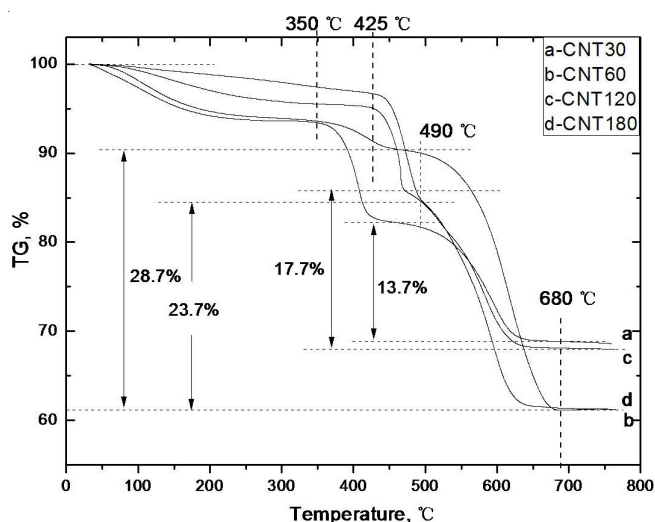


Fig. 3. TG curves of synthesized CNTs for different reaction time (a) CNT30, (b) CNT60, (c) CNT120 and (d) CNT180

The usual method to estimate the quantity of the deposited carbon during decomposition of small hydrocarbon molecules on metal ion-containing catalysts by CCVD is calculated as follows:

$$\text{Carbon yield (\%)} = \frac{(m_{\text{tot}} - m_{\text{cat}})}{m_{\text{cat}}} \times 100$$

where  $m_{\text{cat}}$  is the initial amount of the catalyst (before reaction) and  $m_{\text{tot}}$  is the total weight of the sample after reaction. The use of TG data allows for the determination of the deposited carbon. The results for the synthesized CNTs by different contents of Fe-supported zeolite and by the catalyst sample FeNaX2 for different reaction time are given in Table-1. These results can find some confirmations from former analysis.

TABLE-1  
CARBON YIELD AND QUALITY OF SYNTHESIZED  
CARBON NANOTUBES (CNTs)

Catalyst sample	Carbon yield (%)	Raman ratio ( $I_D/I_G$ )
CNT-FeNaX0	37.1	0.89
CNT-FeNaX1	43.2	0.83
CNT30	36.2	0.89
CNT60	52.9	1.20
CNT120	39.6	0.59
CNT180	58.2	0.85

In addition to TEM and TG analyses, Raman spectra were also taken for the CNT samples. According to a previous work<sup>21</sup>, for samples CNT-FeNaX0, CNT-FeNaX1 and CNT-FeNaX2, there are two apparent peaks at the wavelengths 1280 and 1590  $\text{cm}^{-1}$ , which were identified as D- and G-bands, respectively. The G-band represents the tangential stretching ( $E_{2g}$ ) mode of graphite and is related to the vibration of  $sp^2$ -bonded carbon atoms in a two-dimensional hexagonal lattice. The D-band was associated with the disordered,  $sp^3$ -hybridized carbon present as impurities and dispersive defects in the graphitic sheets<sup>23</sup>. Close to the D-peak of samples CNT-FeNaX0 and CNT-FeNaX1, there is a side peak at *ca.* 1332  $\text{cm}^{-1}$ , which is seen in a previous study<sup>24</sup> as the diamond  $sp^3$  peak and does not exist in the spectrum of sample CNT-FeNaX2. In addition, a broad peak at around 1060  $\text{cm}^{-1}$  (T peak) is shown in CNT-FeNaX0 and CNT-FeNaX1 much higher than in CNT-FeNaX2, which represents the amorphous carbon<sup>25</sup>. This result is in accordance with the former TG analysis. In addition, the relative intensity ratio of the D- to G-bands reveals the degree of disorder in the graphite sheets and they can be used as a measure of the crystallinity of the synthesized CNTs. In present work, the ratios (Table-1) of the D- to G-bands were similar to those reported in the literature (0.7-1.3) for MWNTs conventionally synthesized by CCVD<sup>26</sup>.

Fig. 4 shows Raman spectra of CNT samples, CNT30, CNT60, CNT120 and CNT180. Obviously, D- and G-bands for them are shown around the wavelength of 1280 and 1590  $\text{cm}^{-1}$ , respectively. The relative intensity ratios of the D- to G-bands are shown in Table-1, with the CNTs synthesized for 2 h having the lowest value, indicating that they have the highest crystallinity. Despite that, Fig. 4 shows a broad D peak for CNT30, CNT60 and CNT180, which indicates the existence of defective graphitic layers on the wall surfaces, like the diamond<sup>24</sup> at *ca.* 1332  $\text{cm}^{-1}$ . There are also some small and complex bumps in the spectra for CNT30, CNT60 and CNT180 around the wavelength 1060  $\text{cm}^{-1}$  which is identified in the study<sup>25</sup> as the amorphous carbon, which is in accordance with the former TEM and TG analysis.

It is noted that except for a sudden increase at 1 h, the intensity of D peak decreases with the prolonged reaction time, indicating that defect content is larger when the reaction



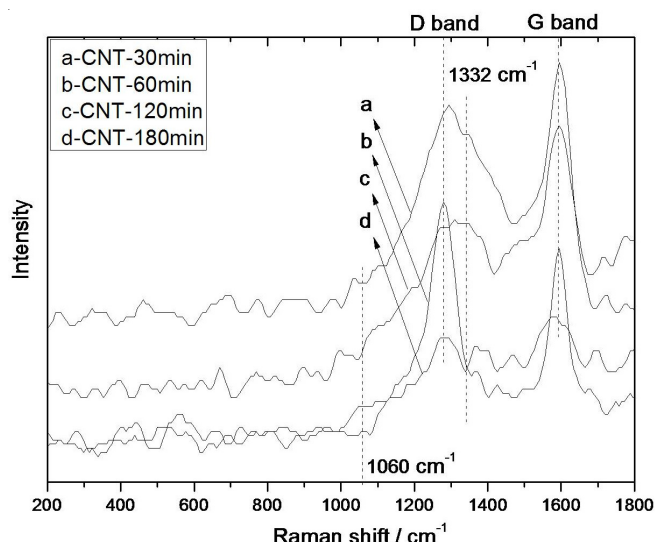


Fig. 4. Raman spectra of synthesized CNTs by catalyst FeNaX2 for different reaction time (a) CNT30, (b) CNT60, (c) CNT120 and (d) CNT180

proceeds for 1 h; the G peak stops keeping single and sharp until the reaction is carried out for 3 h, when it becomes broader and shorter and also has a side peak, indicating that the CNTs obtained after much longer reaction time may have a weaker crystallinity.

### Conclusion

Multi-walled carbon nanotubes (MWNTs) were synthesized by CCVD using Fe-supported zeolite as the catalyst. After 1 h reaction, quite a number of CNTs had inner and outer diameters both below 10 nm<sup>21</sup>. With increasing iron contents in the zeolite, the carbon yield shows a monotonic increasing tendency, reaching 52.9 % when the iron content is up to 6.72 wt. %. In addition, with prolonged reaction time such as 0.5, 1.0, 2.0 and 3.0 h, the inner diameter of the CNTs remained constant while the outer diameter became thicker and thicker, with the carbon yield after the reaction of 3 h reaching 58.2 %. This allows the zeolite to be a container for catalysts and as a guide template for MWNT growth. All CNTs showed two apparent peaks at the wavelengths 1280 and 1590 cm<sup>-1</sup>, which were identified as D- and G-bands, respectively. The CNTs obtained after much longer reaction time may have a weaker crystallinity.

### ACKNOWLEDGEMENTS

This work was supported by Research Foundation from Hanseo University in 2009. The authors are grateful to all staffs in the University for financial support.

### REFERENCES

1. S. Iijima, *Nature*, **354**, 56 (1991).
2. P.J.F. Harris, Cambridge University Press, Cambridge (2001).
3. S.B. Sinnott and R. Andrews, *Crit. Rev. Solid State Mater. Sci.*, **26**, 145 (2001).
4. P.M. Ajayan, *Chem. Rev.*, **99**, 1787 (1999).
5. M.S. Dresselhaus, *Nature*, **391**, 19 (1998).
6. C. Liu, Y.Y. Fan, M. Liu, H.T. Cong, H.M. Cheng and M.S. Dresselhaus, *Science*, **286**, 1127 (1999).
7. S.S. Fan, M.G. Chapline, N.R. Franklin, T.W. Tombler, A.M. Cassell and H.J. Dai, *Science*, **283**, 512 (1999).
8. M. Fuhrer, H. Park and P.L. McEuen, *IEEE Trans. Nanotechnol.*, **1**, 78 (2002).
9. T. Guo, P. Nikolaev, A. Thess, D.T. Colbert and R.E. Smalley, *Chem. Phys. Lett.*, **243**, 49 (1995).
10. M. Endo, K. Takeuchi, K. Kobori, K. Takahashi, H. W. Kroto and A. Sarkar, *Carbon*, **33**, 873 (1995).
11. K.P. De Jong and J.W. Geus, *Catal. Rev.-Sci. Eng.*, **42**, 481 (2000).
12. H. Dai, A.G. Rinzler, P. Nikolaev, A. Thess, D.T. Colbert and R.E. Smalley, *Chem. Phys. Lett.*, **260**, 471 (1996).
13. K. Hernadi, A. Fonseca, J.B. Nagy, D. Bernaerts, A. Fudala and A.A. Lucas, *Zeolites*, **17**, 416 (1996).
14. W.Z. Li, S.S. Xie, L.X. Qian, B.H. Chang, B.S. Zou, W.Y. Zhou, R.A. Zhao and G. Wang, *Science*, **274**, 1701 (1996).
15. K. Hernadi, A. Fonseca, J.B. Nagy, D. Bernaerts and A.A. Lucas, *Carbon*, **34**, 1249 (1996).
16. Z. Konya, I. Vesselenyi, K. Lazar, J. Kiss and I. Kiricsi, *IEEE Trans. Nanotechnol.*, **3**, 73 (2004).
17. I.J. Kim and H.J. Lee, *Key Eng. Mater.*, **280-283**, 891 (2005).
18. M. Karthik, A. Vinu, A.K. Tripathi, N.M. Gupta, M. Palanichamy and V. Murugesan, *Micropor. Mesopor. Mater.*, **70**, 15 (2004).
19. H.J. Lee and I.J. Kim, *J. Eur. Ceramic Soc.*, **27**, 561 (2007).
20. S. Esconjauregui, M. Caroline, Whelan and K. Maex, *Carbon*, **47**, 659 (2009).
21. W. Zhao, D.N. Seo, H.T. Kim and I.J. Kim, *J. Ceramic Soc. Japan*, **118**, 983 (2010).
22. C.J. Lee, J.H. Park, Y. Huh and J.Y. Lee, *Chem. Phys. Lett.*, **343**, 33 (1999).
23. L.D. Shao, G. Tobias, C.G. Salzmann, B. Ballesteros, S.Y. Hong, A. Crossley, B.G. Davis and M.L.H. Green, *Chem. Commun.*, 5090 (2007).
24. A.C. Ferrari and J. Robertson, *Phys. Rev. B*, **63**, 121405 (2001).
25. A.C. Ferrari and J. Robertson, *Phys. Rev. B*, **64**, 075414 (2001).
26. K. Kwok and W.K.S. Chiu, *Carbon*, **43**, 437 (2005).